Conference on Modelling Fluid Flow (CMFF'25)
The 19th International Conference on Fluid Flow Technologies
Budapest, Hungary, August 26 - August 29, 2025

A CFD STUDY ON THE EFFECT OF DEFORMABLE BLADES ON CENTRIFUGAL PUMP PERFORMANCE

Csaba HŐS[1], Balázs ERDŐSI[2]

[1] Corresponding Author. Department of Hydrodynamic Systems, Faculty of Mechanical Engineering, Budapest University of Technology and Economics. Műegyetem rkp. 3., D building, 3rd floor, H-1111 Budapest, Hungary. Tel.: +36 1 463-2216, E-mail: cshos@hds.bme.hu
[2] Department of Hydrodynamic Systems, Faculty of Mechanical Engineering, Budapest University of Technology and Economics. Tel.: +36 70 406-0886, E-mail: erdosi8080@gmail.com

ABSTRACT

This paper uses CFD studies to investigate the effect of passively deforming blades on the flow field, head and efficiency of a centrifugal pump. Impellers with constant blade thickness and width have been considered and mounted to the back shroud with joints at one-third and two-thirds of the blade length. Two different impeller geometries with varying blade thickness and material properties were investigated with two-way coupled numerical fluid-structure-interaction simulation. Not only the standard hydraulic parameters (flow rate, head, input power) were recorded, but the blade deformation was also studied. This paper provides a detailed analysis of the flow field, separation zones and loss mechanism, and the effect of blade deformation. The findings provide headways for further investigations to optimize the impeller's geometry to enhance the turbomachine's operating parameters.

"Keywords: Centrifugal pump, CFD, Flexible blades, Fluid-structure-interaction, Radial flow impeller"

NOMENCLATURE

Latin letters

D	[m]	impeller diameter
H	[m]	head
I	[J/kg]	rothalpy
N_{blade}	[-]	number of blades
P	[kW]	input power
Re	[-]	Reynolds-number
Q	[m^3/s]	flow rate
c	[m/s]	absolute velocity
g	[m/s^2]	gravitational acceleration (9.81)
n_q	[-]	specific speed
r	[m]	impeller radius
u	[m/s]	circumferential velocity
w	[m/s]	relative velocity
y^+	[-]	dimensionless wall distance

Greek symbols

β	[°]	blade angle
δ	[m]	boundary layer thickness
η	[-]	hydraulic efficiency
ρ	[kg/m^3]	density

Subscripts and Superscripts

1	quantities at the leading edge
2	quantities at the trailing edge
m,u	meridional and circumferential component
n	nominal value
ss,ps	suction side and pressure side

1. INTRODUCTION

A significant part of the electricity generated in power plants is used to drive pumps (e.g. drinking water pumps). As a result, it is crucial that these machines can be operated with the highest possible efficiency. The impellers of these machines are usually designed for a single operating point. In real-world conditions, though, operating the machine at other operating points is necessary. In such cases, the increased flow separation on the blades causes the significant growth of the flow losses, which results in a reduction of the efficiency.

In the case of axial flow machines, one possible way to improve efficiency is to change the blade angle. However, this option is not available for radial machines. This paper investigates the viability of a novel approach. The idea is that better efficiency could be achieved at off-design conditions if the blade of the impeller would be passively deformed in a suitable way. Considering that both the pressure difference on the two sides of the blade and centrifugal force act on the blade, the net force causes a passive deformation in the blade shape. The main aim of the investigation is to make this deformation such that it reduces the flow separation.

This may result in an increase in the efficiency of the machine. Research approaches studying the effect of deforming blades can be found in the literature. The previous studies mostly investigate axial-flow machines, especially ones that move air, while the main aim of this actual study is to investigate the use of flexible blades in case of pumps. Such an example of an axial fan with flexible blades can be seen in [1], where piezoelectric ceramic macroscale composite actuators are embedded in the blade of an axial compressor. These actuators are used to achieve deformation and reduce the flow losses. The actuators are used to adjust the twist and the turning of the blade simultaneously. Further approaches are described in [2], that combine the method using piezoelectric actuators in with active flow control. In this case, the flow control means injecting or extracting a flowing medium into or from the boundary layer.

Flexible blades using shape-memory alloys (SMA) were also investigated in different studies, which method allows a greater blade deformation. The more the blade angle at the leading edge can adapt to the actual operating point, the more flow loss emerges due to flow separation. This approach is also found in [3], where an automotive cooling fan is analysed. This describes a method using coupled numerical Fluid-Structure-Interaction (FSI) simulation, like the one used in this actual research. Furthermore, laboratory measurements in a wind tunnel and custom-built measurement equipment were also considered. In the case of study described in [3], however, the changed geometry of the blade resulted in a higher available pressure ratio for the same flow rate but lower efficiency of the ventilator. The effect of the SMA in aerospace applications is investigated in [4], while a study of an expandable-impeller pump is described in [5]. Since the expandable impeller has significant deformation, so the simulation of the fluid-structure interaction had to be made. The structural deformations were time dependent according to [5]. A novel approach can be seen in [6] and [7], that investigates NACA 63-418 profile with flexible trailing edge. The authors of these papers considered both measurement and FSI-simulation and detected significant change in the drag coefficient of the wind turbine. As it can be seen in the literature, the flexible blades of a turbomachine can significantly affect the flow parameters. However, centrifugal pumps were less studied yet.

2. SIMULATION METHODOLOGY

2.1. The hydraulic pre-design of the impellers studied

The geometries of the studied impeller blades were designed with the method of the complex potentials, assuming ideal flow. The blade itself can be considered as a streamline. The design parameters of these impellers are written in Table 1.

Table 1. The design parameters of the studied impellers (with the number of blades)

Geom.	$H\ (m)$	Q (l/s)	n_q (1)	N_{blade}
A	40	30.1	1440	5
B	16	2.833	2345	8

The first one (model *A*) is a larger impeller with also a larger distance between two blades. Therefore, higher deformation could be allowed. The second one (model *B*) is a smaller impeller to be built into a measurement equipment in the future. Besides, its blade number is closer to the ideal (according to empirical formulas) than the first one. A more detailed analysis was done on impeller A, and a less detailed analysis was done on impeller B in this study. However, a half-numeric method was also tested on impeller *B* to reduce the computational cost. The impeller *A* was studied with a blade width 3 mm and is made from steel ($E = 210$ GPa). In the case of the impeller geometry *B*, an impeller made from Aluminium ($E = 68$ GPa) and with 1.5 mm blade width and one made from Acrylonitrile styrene acrylate [ASA], (3D-printed, $E = 1.92$ GPa) and with 2.5 mm blade width were studied. The impeller blades are mounted to the back shroud with joints at one-third and two-thirds of the blade length.

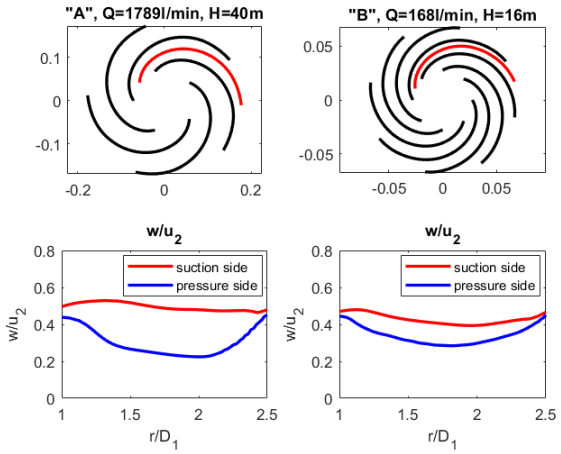

Figure 1. The impeller geometries designed: the A (left) and the B (right) geometries (a streamline in both impellers are marked with red)

It is practical to calculate the relative velocity on the suction and pressure sides of the blade to get the pressure difference between them using Bernoulli's equation. However, according to the previous experiences, these results differ significantly from the results of the simulation the due to the flow separation. So, the study focuses only on the FSI-simulation methods. The pre-design method cannot consider viscous losses too. To calculate the Reynolds number, the flow speed can be evaluated with the relative velocity averaged on the two side of the blade (Figure 1). The relative velocity should be nearly constant along the full length of the blade.

2.2. The pre-processing of the CFD simulation

The main dimensionless parameters describing the turbulence of the flow and the width of the boundary layer are written in Table 2. (Average Reynolds-number of the pump, y^+ on suction and pressure side of the blade, boundary layer thickness.)

Table 2. The main parameters of the three discretized simulation geometries

Geom.	Re (1)	y_{ss}^+ (1)	y_{ps}^+ (1)	δ (mm)
A	7.48*e*5	29.77	53.16	8
B (Alu)	9.52*e*4	39.93	39.93	4.78
B (Asa)	9.52*e*4	16.46	24.69	4.78

The higher Reynolds-number wall turbulence model requires the value of the y^+ between 30 and 300. The mesh of the ASA impeller does not clearly meet this condition; however, it can be allowed for this testing phase of the due to easier meshing. This may lead to imprecise results regarding to flow separation, so further analysis has to be done in the future. The meshes can be qualified with the skewness of their elements (Table 3.). The intolerably deformed elements are usually around the trailing edge of the blade as it can be seen on Figure 2 (bottom-left). This is due to the blade being relatively thin, and the trailing edge being sharp compared to the size of the flow field.

Table 3. The skewness and the average quality of the elements of the simulation geometries

Geom.	min.	max.	avg.	avg. q.
A	$3e-4$	0.94	$7e-2$	0.91
B (Alu)	$6e-4$	0.71	0.11	0.67
B (Asa)	$9e-4$	0.55	$8e-2$	0.9

The simulation was made in *Ansys CFX*. On the sides of the flow field, periodic boundary condition was defined (Figure 2, blue). The blade (Figure 2, yellow) and the boundaries on the top and the bottom of the flow field (Figure 2, grey) can be considered as a no slip wall, resulting in a closed impeller.

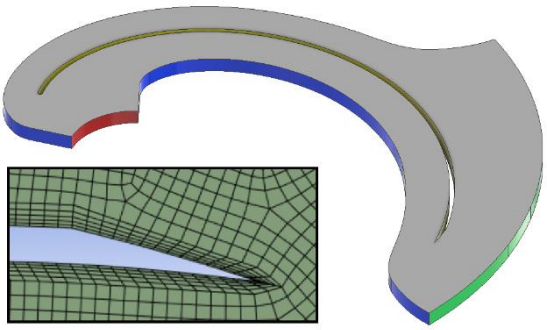

Figure 2. The flow field and the mesh around the trailing edge of the blade (in case of impeller A)

2.3. The FSI simulation

The FSI simulation is a coupled two-way Fluid-structure-action simulation, which is essential for investigating the blade deformation due to the flow and its reaction to the flow region. The mechanical finite-element model of the blade is also discretized (Figure 3). According to Table 3., the minimum, maximum and average value of the skewness and the overall average mesh quality are acceptable in all cases. To run the CFD simulation a rotating flow domain and SST turbulence model was considered.

The mountings can be rigid (like the blade had been welded to the back shroud in two points). This method means the use of cylindrical constraints on the mountings of the blade that restrain all degrees of freedom. The other approach is that the mountings allow rotational movement (like riveted mounting) using cylindrical constraints allowing rotation and adding remote displacement constraint too.

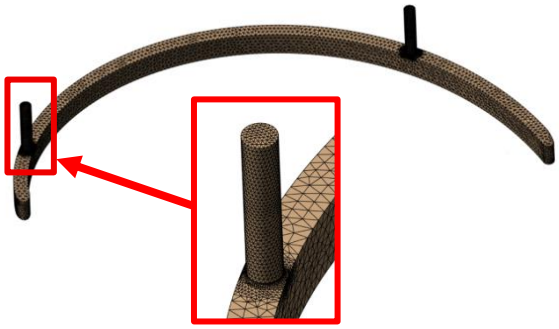

Figure 3. The mechanical model and the place of the mounting

In the case of FSI simulation, only the shape of the blade (Figure 2, yellow) can change; the deformation of every other boundary region of the flow field should be unspecified. Considering the rigid bladed impeller will be important too in the future calculations: it can be managed by running only a CFD simulation on the designed flow field, neglecting the deformation of the blade. The FSI simulation was performed with the help of *Ansys System Coupling* software. Only steady-state simulations were run. Knowing that CFD simulations may be inaccurate in off-design points, the results should be considered carefully, future simulations are recommended. Furthermore, the next phase of this actual research plan is measurement in laboratory, which can give more accurate results in off-design conditions too.

2.4. The Grid sensitivity analysis

Each geometry was investigated with more grids, and the comparison between them was made by the help of the hydraulic parameters of the pump. The sensitivity was studied with only running a CFD simulation on the flow field, without FSI.

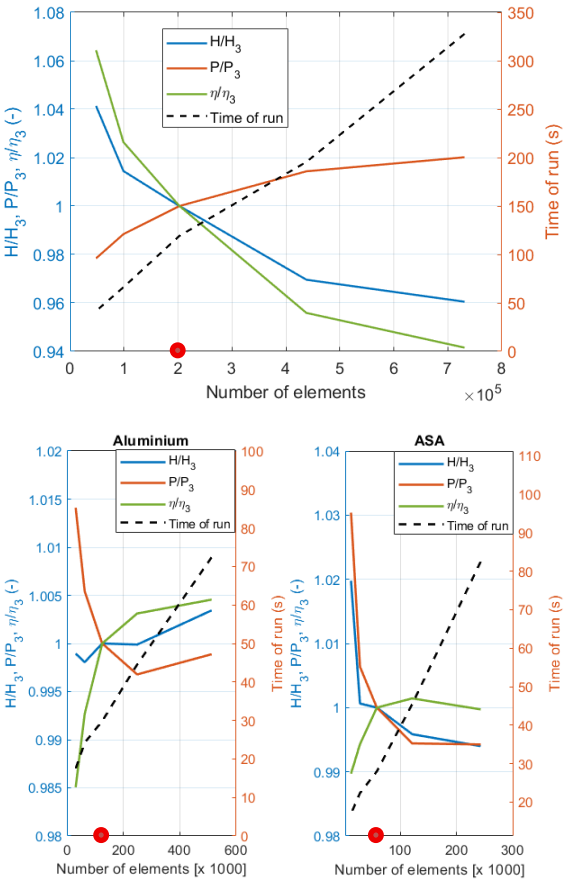

Figure 4. The hydraulic parameters of the impeller *A* (upper) and impeller *B* (lower) got from simulations with different grids

As Figure 4 shows, the hydraulic parameters, such as head, input power and hydraulic efficiency, do not change significantly using different grids. However, the time of a CFD simulation run (or one step of the FSI simulation) is almost directly proportional to the number of elements. As a result, the meshes marked with a red dot (and indexed as the 3rd) on Figure 4 have been chosen for each geometry, which resulted in both satisfactory time of running a simulation and accuracy. (To make visualization easier, the hydraulic parameters were proportioned to the results got with the marked meshes).

3. RESULTS IN CASE OF IMPELLER *A*

3.1. The hydraulic characteristics

As impeller model *A* allowed the largest blade deformation, the difference between the hydraulic parameters of the rigid and the flexible blade was the most significant in this case. (The impeller *B* was made basically to a future measurement equipment.)

The characteristic curves will be usually plotted as function of the relative flow rate: the ratio of the actual and the nominal flow rate. When results are plotted, the continuous lines are trendlines in the following chapters.

Firstly, the head characteristics can give information about the effect of the flexible blade. The numerically calculated head curve of the rigid-bladed impeller should be compared with the theoretical head characteristics.

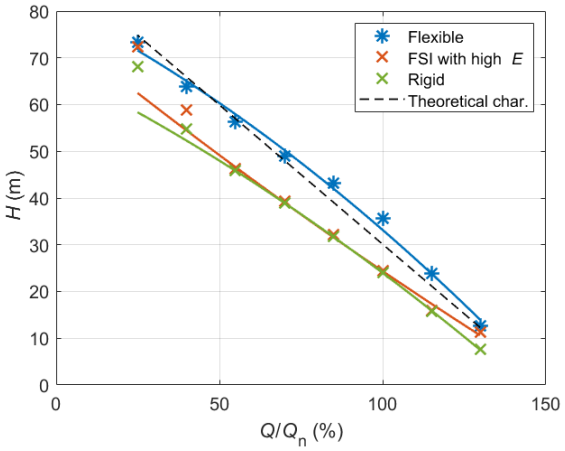

Figure 5. The head characteristics of the rigid and flexible impeller blades and the theoretical head characteristics with a rigid impeller with infinitely many blades

All the impellers investigated was assumed with blades that have constant blade thickness and width. The theoretical head of the studied impeller can be approximated as follows according to empirical equations:

$$H_{t\infty} = -59{,}607\,\frac{Q}{Q_n} + 89{,}717\ (\mathrm{m}) \qquad (1)$$

The head characteristics of the flexible blade run significantly higher than the one of the rigid blades according to Figure 5. The reason of this is the deformation of the impeller circumference (the blade's trailing edge; see section 3.2). The overall deformation of the blade depends on the Young's modulus of the blade material and the geometry of the blade, especially the blade width. In the case of the actual study, linear elastic model can be considered. This means that the deformation is directly proportional to the force applied on the blade and the proportion factor is the Young's modulus

It was also taken to consideration, that the improvement in the pump head is due to the blade deformation and not just numerical error. A simple method was developed: an FSI simulation with the Young's modulus set high (usually over $2 \cdot 10^4$ GPa) that results practically in a rigid blade. If the results of this simulation ran close to the results of the rigid simulation (only CFD simulation without FSI), the change in the hydraulic parameters can be considered as the result of the flexible blades. The overall head has therefore increased. However, this does not necessarily imply an increase in the efficiency and a decrease in flow loss due to flow separation.

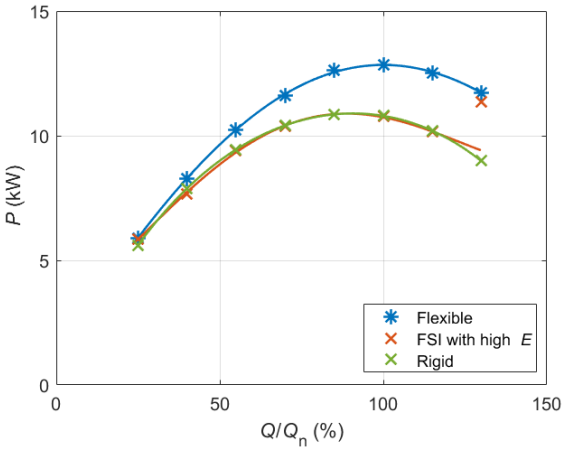

Figure 6. The input power characteristics of the rigid and flexible impeller blades

The input power of the pump should also be taken into consideration, which can be seen on Figure 6. These results are favourable because the input power appears to be higher due to the flexible blading and not a numerical error, as it could be seen in case of the head. It is difficult to calculate the characteristic curves of the recorded power analytically; the hydraulic efficiency curves should be taken into consideration instead (Figure 7).

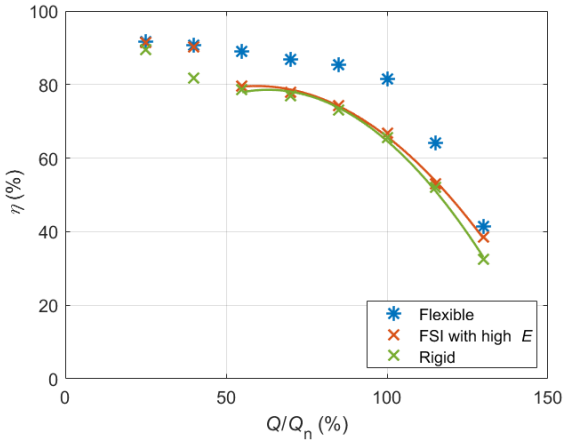

Figure 7. The hydraulic efficiency curves of the rigid and flexible impeller blades

The efficiency of flexible blades is approximately 5-25% better than rigid blades. This was one of the main goals of the research. The efficiency improved mainly for medium flow rates. Since this study investigates only the impeller (the losses of the volute chamber or the mechanical losses were not considered), the efficiency depends only on the friction and the losses due to flow separation. This is, in fact, the hydraulic efficiency of the pump. To investigate these in more detail, and to interpret the improvement in efficiency, it is necessary to carry out a flow chart analysis too, which is discussed in more detail in section 3.3.

3.2. The blade deformation

To analyse the effects of the blade deformation, the velocity triangles at the leading edge and the trailing edge of the blade should be considered. The Figure 8 shows the velocity triangles.

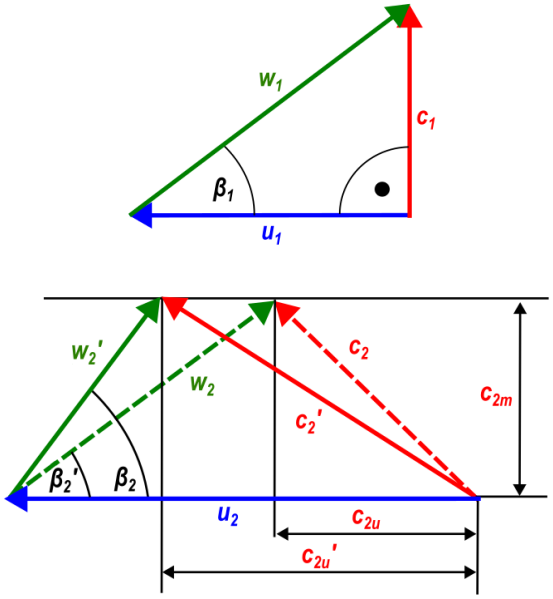

Figure 8. The velocity triangles

Considering Euler's turbine equation:

$$H = \frac{c_{2u}u_2 - c_{1u}u_1}{g} \qquad (2)$$

The value of the head of the pump could be improved in the following cases neglecting the viscous losses and considering only the Equation (2):

- The absolute velocity at the leading edge has less or no circumferential component. The ideal case is that the absolute velocity vector is perpendicular to the circumferential velocity; therefore, the circumferential component of the absolute velocity is zero. This means that the absolute velocity has only a meridional component that can be calculated analytically. Knowing this and the circumferential velocity, the optimal blade angle can be calculated too, as it can be seen on the upper part of the Figure 9 too.
- The circumferential component of the absolute velocity at the trailing edge is higher. This means that the blade angle at the trailing edge should be as high as possible, and as a result, the angle between the circumferential and absolute velocities should be low. This implies that the circumferential component of the absolute velocity is high, next to the same meridional component of the absolute velocity.

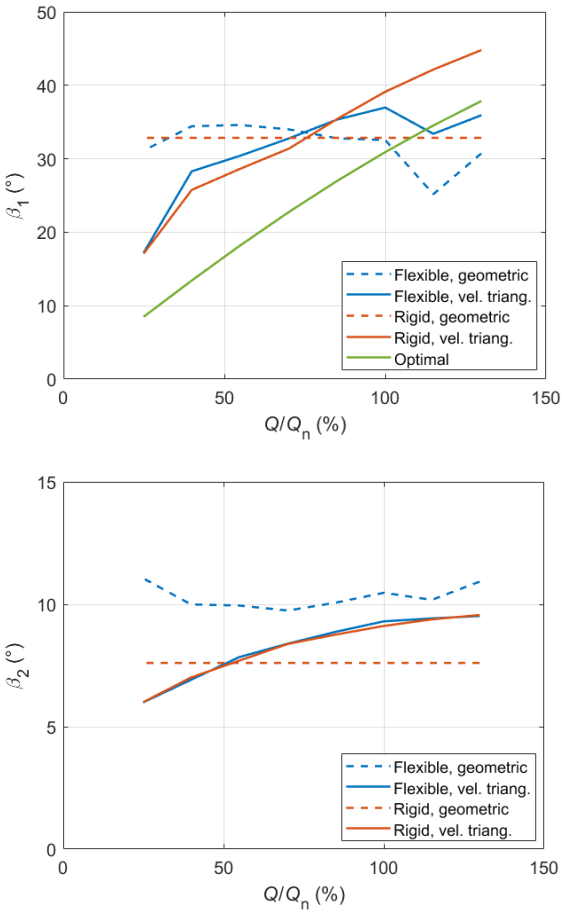

Figure 9. The blade angles at the leading (upper) and the trailing (lower) edge (flexible and rigid blade)

The Ansys CFX post-processor can measure the deformed geometric blade angle. The blade angle can be calculated from the velocity triangle can be known from the simulation results. The upper part of Figure 9 shows that the deformation of the blade angle at the leading edge in the case of flexible blade is opposite to the desired direction. This is due to the flow separation on the leading edge, which results in a suction zone. This zone makes the blade deform opposite to the required direction. The goal would be having the geometric blade angle as close to the optimal as possible and reducing the flow separation.

However, this does not mean that the head achieved get significantly lower as it could be seen in Chapter 3.1. The equation (2) includes the circumferential velocity, which velocity is significantly higher at the trailing edge than at the leading edge. As a result, the deformation of the trailing edge should affect the head of the pump more significantly, because the circumferential velocity is significantly higher at the trailing edge than the leading edge. The characteristics of the deformation and the blade angle are consistent with the head curve, because the higher β_2 angle of the flexible blade resulted in the growth of the pump head.

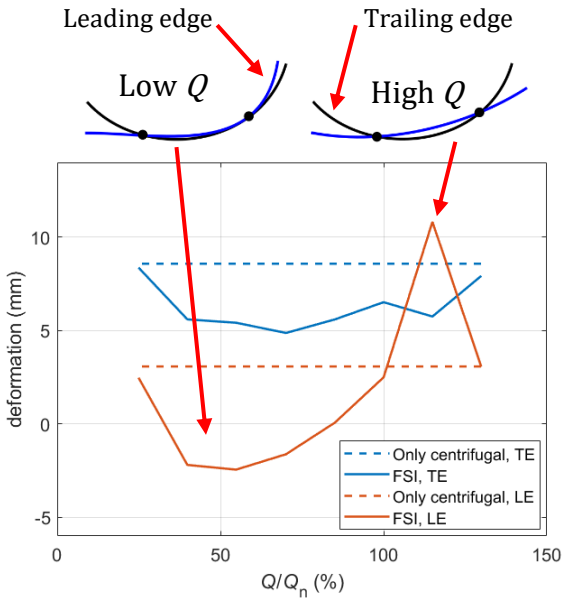

Figure 10. The effect of the centrifugal force and the flow on the deformation of the blade (the deformed blade geometry is blue)

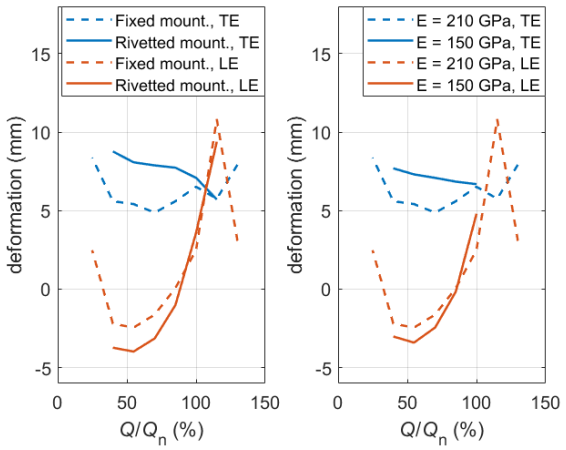

Figure 11. The effect of the mounting (l) and the lower Young's modulus (r) on the deformation

As Figure 11 shows, neither the rivetted mounting nor the more flexible blade material significantly affected the deformation at the blade's edges. This means that the fixed mounting should be preferred to the first testing period of the research: it is easier to manufacture and numerically more stable, too. The more flexible blade material should be investigated with another impeller though, which is written in section 4. It was also studied if the field of the centrifugal force itself can lead to the same amount of deformation as it would be combined with the flow. This would be true, if the FSI simulation gave approximately the same deformation, as the centrifugal force itself. It has been proven to be false, (see Figure 10). As it can be seen, the effect of the flow leads to significantly different deformation.

This is important, because if it was not, an easier simulation without FSI could have been made, reducing computational cost. In the future, a fan impeller should be also taken to consideration, because in this case, the effect of the centrifugal force may be more significant.

3.3. The analysis of the flow field

The blade deformation is a direct answer to the increase in the head of the pump as it could be seen in Chapter 3.1 and 3.2. (therefore, an increase in the input power, too). However, a more detailed study of the impeller flow field is needed to investigate the improved hydraulic efficiency.

The rothalpy, as an energy-dimension quantity, should be taken into consideration. This will be used to investigate the flow losses and, consequently, the efficiency relations for the different simulations. Note that in a stationary coordinate system, the total pressure would be the appropriate variable to study the losses. Neglecting the potential energy and assuming the constant temperature of the fluid, the rothalpy can be written as follows:

$$I = \frac{p}{\rho} + \frac{w^2}{2} - \frac{u^2}{2} \tag{3}$$

In this case, the rothalpy, that describes the losses can decrease due to the work of the shear stresses or dissipation and heat transfer from the flow. The decrease in the rothalpy in the flow field is the following can be seen on Figure 12. This is shown in the case of 85% relative flow rate because this shows the most significant difference between the rigid and the flexible blade.

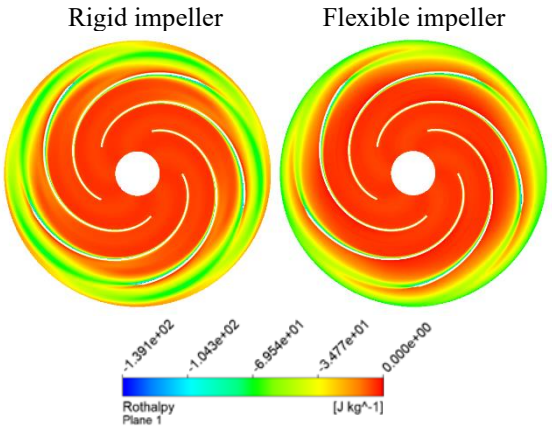

Figure 12. The loss of the rothalpy in the flow field: colour blue means high flow losses

Figure 12. shows that the zones with a higher loss in the rothalpy is wider in case of rigid blade. This implies higher loss due to flow separation, especially around the trailing edge of the blade. The lower this flow separation zones could be, the higher would be.

4. RESULTS IN CASE OF IMPELLER *B*

The impeller geometry *B* was tested with either blade made from Aluminium or 3D-printed ASA for experimental studies to be carried out in the future.

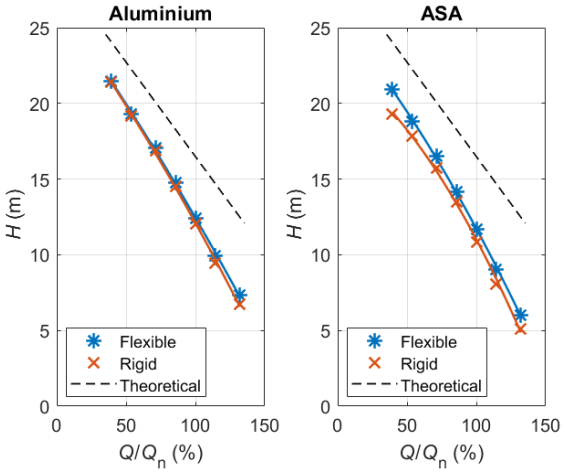

Figure 13. The head characteristics of the Aluminium and ASA-bladed impellers

As Figure 13 shows, the real head characteristics are significantly lower than the theoretical curve compared to the steel impeller. The reason of this is that the blade width of the ASA and the Aluminium blade compared to the impeller diameter is significantly higher than the one made from steel. The trailing edge of these blades is filleted, too, not as sharp as the steel one (see Figure 2). This results in a higher flow separation. Furthermore, the flow separation can affect the characteristics even more due to the higher number of blades.

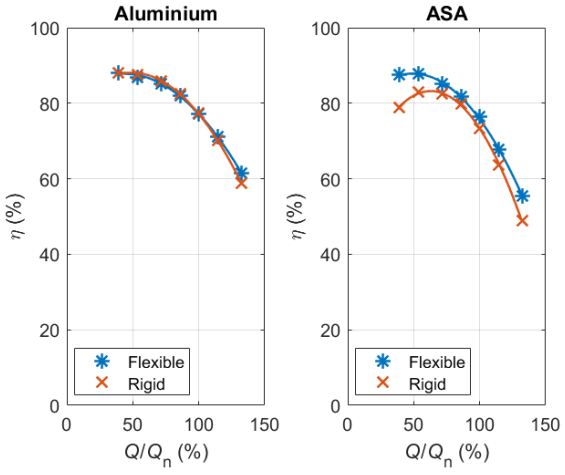

Figure 14. The efficiency characteristics of the Aluminium and ASA-bladed impellers

The ASA blade is more flexible than the Aluminium one. Consequently, bigger improvement can be achieved with it in efficiency. This is even more significant in off-design points (Figure 14).

One of the research goals is exactly this: designing a flexible blade, that improves the hydraulic efficiency in off-design operating points.

The FSI simulation's main disadvantage is its significantly high computational cost, especially with high mesh element numbers. To make the algorithm faster, a half-numeric method was also tested. This means that the net force due to the flow and the centrifugal force field are calculated only in one iteration step. This force is applied to the analytical model of the blade, which means a beam fixed in two points. Solving the differential equation of a flexible beam would be a boundary condition problem that could be solved. However, this method has been proven to resulting in significantly lower deformations than the FSI simulation. The possible cause of this is that the flow separation at the leading edge leads to a pressure drop, and high suction force, as it can be seen in Figure 15. Due to the deformation caused by this force, the higher the deformation at the leading edge is (see section 3.2), the higher the flow separation will be. As a result, this method could not be used to further analysis.

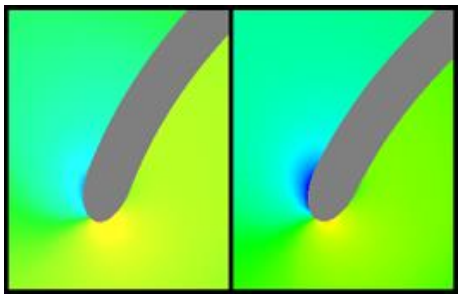

Figure 15. Flow separation zones around the leading edge in the case of rigid blade (left) and deformed flexible blade (right)

5. CONCLUSION

Coupled FSI simulations were used to investigate the effects of rigid and flexible bladed impellers on the hydraulic parameters such as head and efficiency. The flexible impeller increased the efficiency by 10-20% depending on the flow rate, and 15% increment was recorded in case of impeller *A* in the best-efficiency point. In addition, due to the deformation, the head increased. In all cases, the trailing edge of the blade is slightly displaced towards the pressure side, while the leading edge is displaced towards the suction side at lower flow rates and towards the pressure side at higher flow rates. This is quite unfavourable; the blade should deform in such way that the leading edge moves towards the optimal direction. This can be made, for example, by actuators ([1] [3]). However, this method would result in a significantly more difficult and more expensive to manufacture impeller than the passively deformable one. A significant part of the deformation is due to the centrifugal force, but the effect of pressure distribution is also not negligible. It can be stated that the rothalpy remains approximately constant according to the theoretical value between the two blades, but there are separation zones on the blade, too. These depend on the flow rate and the flexibility of the blade. However, the present study of the flow field does not allow a more precise and detailed explanation of the improvement in efficiency, so this requires further analysis such as more accurate simulations and experimental studies. It is also important to make the blade as thin as possible to earn the best efficiency and more streamlined design.

The inaccuracy of the simulation is partly due to the less accurate mesh and numerical scheme. However, a more accurate scheme would made the meshing procedure significantly more difficult. The simulation converges relatively slowly, especially in further distance from the design point, and does not converge at all flow rates. A possible solution to this problem could be a transient simulation, but the computational capacity requirement of this is significantly higher.

REFERENCES

[1] Seidler, M., Bode, C. and Friedric, J., 2024, "Effect of Blade Reference Design Variations on the Morphing Capability of a Shape-Adaptive Fan Rotor" *International Journal of Gas Turbine, Propulsion and Power Systems* Vol. 15., Num. 2.

[2] Seidler, M. et. al., 2024, "Combining shape adaptive blades and active flow control in a multi stage axial compressor: a numerical study" *CEAS Aeronautical Journal*, p. 239–253

[3] A. Suman et. al., 2027, „Analysis of the Aerodynamic and Structural Performance of a Cooling Fan with Morphing Blade" International Journal of Turbomachinery Propulsion and Power (2017,2,7)

[4] Hartl, D. J. and Lagoudas, D. C., 2007, „Aerospace applications of shape memory alloys" *Proc. IMechE* Vol. 221 Part G: J. Aerospace Engineering

[5] Campbell, R. L., Paterson, E. G., 2011, „Fluid–structure interaction analysis of flexible turbomachinery" *Journal of Fluids and Structures 27* (2011) 1376–1391

[6] Daynes, S. and Weaver, P. M., 2012, „A morphing trailing edge device for a wind turbine" *Journal of Intelligent Material Systems and Structures* 23(6) 691–701

[7] Daynes, S. and Weaver, P. M., 2012, „Design and testing of a deformable wind turbine blade control surface" *Smart Materials and Structures* 21 (2012) 105019 (10pp)